Intercoupling of free-space radiation to *s*-polarized confined modes via nanocavities

A. Yu. Nikitin,[1,2,a] F. J. García-Vidal,[3] and L. Martín-Moreno[1]
[1]*Departamento de Física de la Materia Condensada and Instituto de Ciencia de Materiales de Aragón, CSIC-Universidad de Zaragoza, E-50009 Zaragoza, Spain*
[2]*A. Ya. Usikov Institute for Radiophysics and Electronics, Ukrainian Academy of Sciences, 61085 Kharkov, Ukraine*
[3]*Departamento de Física Teórica de la Materia Condensada, Universidad Autónoma de Madrid, E-28049 Madrid, Spain*

(Received 12 January 2009; accepted 26 January 2009; published online 12 February 2009)

The interaction of the *s*-polarized waveguide mode in the dielectric layer placed on a metal film with one-dimensional indentations in the metal is studied. The efficiency of the coupling to the out-of-plane radiation is considered. It is shown that varying the parameters of the cavities, the periodical array of resonant indentations can almost totally reflect back the incident waveguide mode or, on the contrary, efficiently transform it into a narrow-directional outgoing beam. An efficient waveguide mode launcher is examined on the basis of the results for Bragg mirror. The differences and similarities between scattering of surface plasmon polaritons and waveguide modes are discussed. © *2009 American Institute of Physics*. [DOI: 10.1063/1.3081457]

Surface waves (SWs) attract a great deal of attention in photonics for their ability to resonantly enhance the interaction of light with nanostructures. It is well known that a flat metal surface supports *p*-polarized SW in the form of surface plasmon polaritons (SPPs). Diffraction of the *p*-polarized wave at nanocavities leads to enhanced transmission,[1] light beaming,[2] SPP launching,[3,4] and Bragg reflection.[5–7] When the incident plane is perpendicular to the axis along which the structure is homogeneous, the SPP-assisted effects only exist for *p*-polarization. However, if a dielectric layer is deposited onto the metal surface, bound modes are present for *s*-polarization in the form of the waveguide modes (DWMs). These modes also enhance numerous diffraction effects. For instance, a periodically perforated metal film surrounded by dielectric slabs displays the enhanced transmission,[8,9] analogously to the SPP-enhanced light transmission[10,11] in *p*-polarization for the uncoated perforated film.

In this letter, we show how to transfer SW-launching effects to the case of *s*-polarization for a two-dimensional geometry. First, we consider the coupling of a normally incident *s*-polarized wave to the DWM due to the presence of a slit, second we study a Bragg mirror for the DWM and, finally, we propose a back-side slit-illumination method to provide localized unidirectional excitation of the DWM.

We use the mode expansion technique to treat the electromagnetic problem[5] considering as many modes as needed in order to achieve convergency. For simplicity, the metal is assumed to be a perfect electric conductor (PEC). In a real metal, the dispersion of DWM would slightly change, resulting in a small shift in the computed scattering spectra. Throughout the manuscript, both the dielectric inside the slit and that of the slab have permittivity $\epsilon=2.25$. We consider dielectric slab thickness 400 nm, so only the fundamental mode propagates in the dielectric waveguide in the spectral region 600–1700 nm. The wavelength dependency of the parallel component of the lowest DWM wavevector $q_w=k_{wx}/g$ (with $g=2\pi/\lambda$) is shown in the inset of Fig. 1. Notice that nanometric scales are chosen here just for convenience. They can be rescaled appropriately for any spectral range since only the ratio of the structure dimensions to the wavelength are crucial.

To start with, let us concentrate on the situation depicted in Fig. 1(a). A *s*-polarized plane wave (electric field along the *y*-direction) impinges normally onto a slit of width *a* drilled

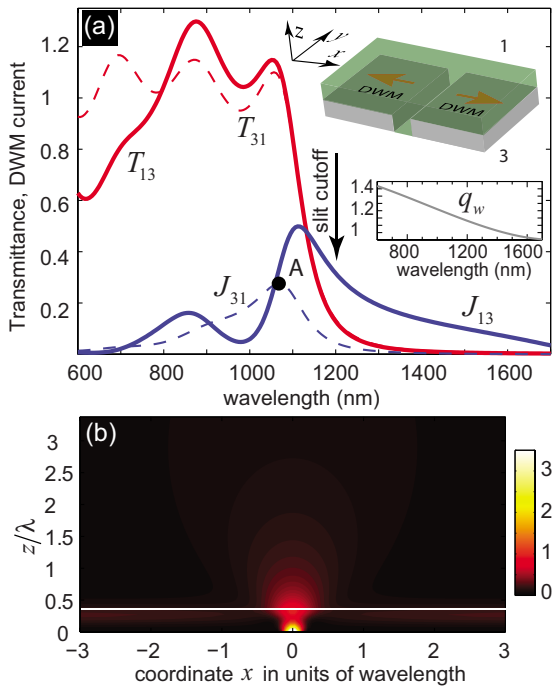

FIG. 1. (Color online) (a) Normalized-to-slit-width spectra of both the transmission *T* and DWM current *J* through a slit filled with glass. The thickness of both metal film and glass slab ($\varepsilon=2.25$) is 400 nm. The slit width is 400 nm. (b) Near-field intensity contourplot at the maximum of J_{31} (point A on the dashed line, $\lambda=1070$ nm), where the slit is centered at $x=0$. Here and in the other figures $z=0$ and horizontal white light are the regions of the glass layer. Inset of (a) shows dispersion curve of the lowest TE mode of the dielectric slab $q_w=q_w(\lambda)$.

[a]Electronic mail: alexeynik@rambler.ru.

in a metal film, on which a continuous dielectric film lies. The indexes of the computed values $T_{\alpha\beta}$ (fraction of energy flux transmitted through the slit) and $J_{\alpha\beta}$ (fraction of energy flux coupled into the DWM) indicate that the wave is incident from the half-space "α," penetrating through the slit into the half-space "β." "1" marks the half-space above the dielectric slab. Both T_{13} and T_{31} present a resonant character at wavelengths slightly smaller that the cutoff one[12] $\lambda_c = 2a\sqrt{\epsilon}$ (1200 nm for chosen parameters). A set of resonant maxima appears when the condition of Fabry–Pérot reflection is fulfilled. For wavelengths larger than the cutoff, the transmission have an exponential decrease due to attenuation of the fundamental mode of the slit, $T \sim f(\lambda)\exp(-2|k_{z1}|h_f)$, where $k_{z1} = \pi/a\sqrt{(\lambda_c/\lambda)^2 - 1}$, h_f is the slit thickness, and a is the slit width. For very long wavelengths, in the region $ga \ll 1$, the transmission spectrum scales as $f(\lambda) \sim (ga)^2$. Notice that this radically differs from the case of the p-polarization, where the slit does not present cutoff and, therefore, the transmission can be high even for small ga. J_{13} and J_{31} also have a resonant behavior. The current is higher when the wave is incident from 1, $J_{13} > J_{31}$, i.e., when the DWM is excited directly, without penetration of the radiation through the slit. The intensity pattern of the field emitted by the slit is rendered in Fig. 1(b). The angular scattering cross section $S_r(\theta)$ has approximately the dependence corresponding to an in-plane electric dipole $S_r(\theta) \sim \cos^2\theta$.

Let us now focus on a different problem: the scattering properties of a DWM by indentations [see Fig. 2(a)]. The reflection coefficient of a single indentation has a nonmonotonic character as a function of the groove width[13] a_i, see Fig. 2(b). In the limit of a small depth [see the case of $h = 40$ nm in Fig. 2(b)], R behaves periodically as $R \sim \sin^2(k_{wx}a_i)$ thanks to interference caused by wave reflection from walls of the indentation (as can be proven within perturbation theory following[14]). However, small cavities do not scatter DWM as efficiently as they do for the SPP in an uncoated metal film. For example, grooves with $h = 40$ nm reflect SPPs about ten times more than they reflect DWM. Such a difference between SPP and DWM comes from the significant difference in their field structure. The SPP electric field is maximal on the metal surface, while the electric field of DWM is very small (exactly zero for PEC). Thus, DWMs are much less sensible to the surface roughness than SPP, and larger scatterers are needed for obtaining appreciable reflection values. For deeper indentations [see the case of $h = 200$ nm in Fig. 2(b)], and especially close to their resonant wavelengths, the reflection coefficient increases and its behavior as a function of a_i/λ does not follow any simple law.

Several equidistantly separated indentations form a Bragg mirror for DWM.[15] The reflection R, transmission T, and out-of-plane scattering S spectra for the DWM impinging onto the Bragg mirror composed of ten indentations are shown in Fig. 2(c). R has a strong maximum close to the wavelengths $\lambda_n = 2Lq_w/n$, where L is the period and the integer n is the order of the band gap. For the chosen parameters, the resonance is better pronounced for the first band gap ($\lambda \simeq 1300$ nm) than for the second one ($\lambda \simeq 800$ nm). This difference is due both to the DWM dispersion and to the scattering cross section of the single indentation with $h = 200$ nm. For the considered geometrical parameters, R increases when λ increases (that is opposite to the case of small a_i/λ, where the Bragg reflection peak of the second band gap can equal or even exceed that of the first one). The out-of-plane emission coefficient S has a wide maximum between the first and the second reflection gaps. The beam emitted by the Bragg mirror can be highly collimated [see Fig. 2(d)]. The spatial near-field distribution illustrates the effect of the Bragg reflection, see Fig. 2(d). As expected, the field does not penetrate into the region to the far end of the mirror.

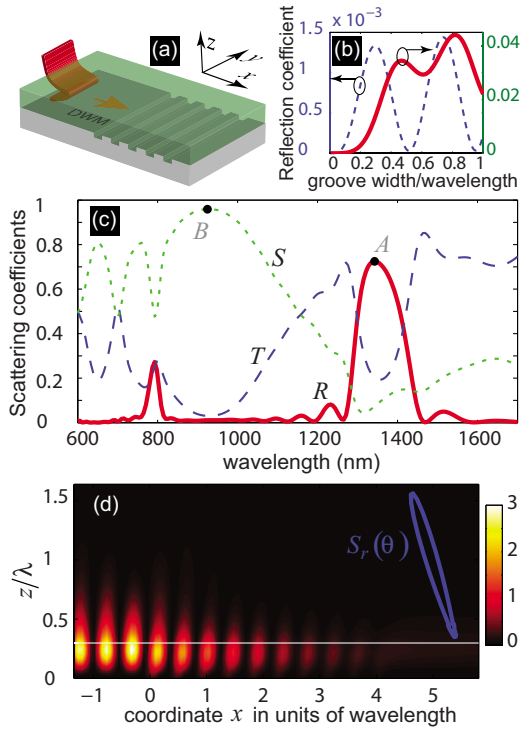

FIG. 2. (Color online) Scattering properties of an incident waveguide mode impinging onto an array of N grooves in the metal. The dielectric slab thickness is 400 nm. (b) Reflection coefficient for a single groove ($N=1$), as a function of groove width and for $\lambda = 1144$ nm. The solid curve is for $h = 40$ nm while the dashed one is for $h = 200$ nm. (c) The DWM reflection R, transmission T, and out-of-plane scattering coefficient S wavelength spectra for the Bragg mirror with $N=10$. The period of the array is $L=600$ nm, the groove depth and width are 200 and 400 nm, respectively. (d) Electric field intensity spatial structure at maximum reflection [point A in (c), $\lambda = 1342$ nm]. The continuous blue curve renders the angular scattering cross-section $S_r(\theta)$ for the wavelength of maximum S [point B in (c), $\lambda = 930$ nm]. The indentations occupy the region $x > 0$, with the center of the first one placed at $x = 0$.

Now, using the previous results and following,[4] we can design a very simple structure to unidirectionally launch DWM with a localized source. Placing the Bragg mirror to the right from the slit in the metal film (at the exit face, which is coated with a dielectric layer), the DWM emerging from the slit to the right side will be mainly backscattered at $\lambda \simeq \lambda_n$. The interference of the reflected DWM with the one propagating to the left from the slit can be tuned by the distance from the slit to the Bragg mirror d. Analogously to the case of SPP, the efficiency coefficient E_R is defined as the ratio between the current intensity of left-propagating DWM with and without the array of grooves. Notice that when $E_R > 2$, the left-propagating DWM carries more current than the total DWM current in the single-slit case, implying that some of the power radiated out of plane has been reimbursed onto the DWM channel. Using the amplitude reflection coefficient of the groove array r_B, the efficiency coefficient can be approximated by a simple expression $E_R \simeq |1 + r_B e^{2ik_{wx}d}|^2$.

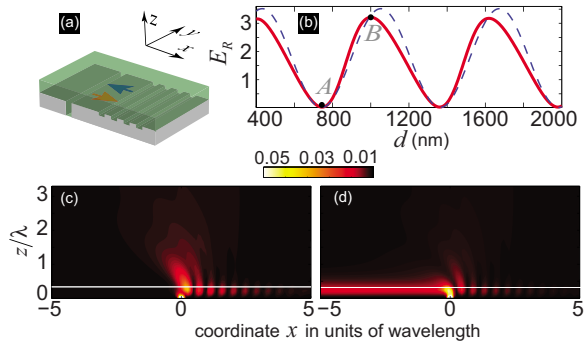

FIG. 3. (Color online) Waveguide mode launcher. (b) Dependency of the efficiency coefficient E_R upon the distance d from the slit to the Bragg mirror at $\lambda=1342$ nm. The solid curve represent the exact calculation, while the dashed curve is obtained with the simplified interference model. The Bragg mirror parameters are the same as in Fig. 2, the slit width is 400 nm. (c) Electric field intensity for the point A in (b). (d) Electric field intensity for the point B in (b). The array extends to the region $x>0$, with the center of the slit at $x=0$.

Figure 3(b) shows E_R as a function of d, obtained with both the full calculation and the simplified analytical model. In the analytical model, we take the Bragg mirror reflection coefficient at the maximum of the spectra in Fig. 2(b), $|r_B|=0.876$ at $\lambda=1342$ nm. The locations of maximum E_R are accurately predicted by the analytical model. To visualize the backscattering of DWM, we have rendered the near-field contour-plots at the point of destructive interference "A" ($d=744$ nm) and constructive interference "B" ($d=1000$ nm). For the configuration B, the enhanced left-side current of DWM is clearly seen, while for A the left-side current is zero. Notice that when $E_R=0$, all radiation is emitted out of plane and the coupling into DWMs propagating in both directions has been totally suppressed, despite using only one Bragg mirror.

To conclude, we have studied the excitation of DWMs by a slit and the scattering of DWM by an array of indentations. The conditions for maximum reflection and out-of-plane coupling have been given. We have found that due to the field structure of DWM (zero at the metal boundary), efficient scattering or excitation of DWM requires larger cavities than for the case of SPPs. Additionally, we have shown how to make a unidirectional launching of the DWM using a slit and a Bragg mirror composed by an array of grooves. These effects could be used for the design of ultra-compact optical devices such as photonic circuits or light-emitting diodes.

The authors acknowledge support from the Spanish MECD under Contract No. MAT2005-06608-C02, EU Project "PLEAS" FP6-2006-IST-034506 and Consolider Project "Nanolight.es."

[1] T. Thio, K. M. Pellerin, R. A. Linke, H. J. Lezec, and T. W. Ebbesen, Opt. Lett. **26**, 1972 (2001).
[2] H. J. Lezec, A. Degiron, E. Devaux, R. A. Linke, L. Martín-Moreno, F. J. García-Vidal, and T. W. Ebbesen, Science **297**, 820 (2002).
[3] P. Lalanne and J. P. Hugonin, Nat. Phys. **2**, 551 (2006).
[4] F. López-Tejeira, S. R. Rodrigo, L. Martín-Moreno, F. J. García-Vidal, E. Devaux, T. W. Ebbesen, J. R. Krenn, I. P. Radko, S. I. Bozhevolnyi, M. U. González, J. C. Weeber, and A. Dereux, Nat. Phys. **3**, 324 (2007).
[5] F. López-Tejeira, F. J. García-Vidal, and L. Martín-Moreno, Phys. Rev. B **72**, 161405 (2005).
[6] A. Drezet, A. L. Stepanov, A. Hohenau, B. Steinberger, N. Galler, H. Ditlbacher, A. Leitner, F. R. Aussenegg, J. R. Krenn, M. U. Gonzalez, and J.-C. Weeber, Europhys. Lett. **74**, 693 (2006).
[7] J. A. Sánchez-Gil and A. A. Maradudin, Appl. Phys. Lett. **86**, 251106 (2005).
[8] A. Christ, S. G. Tikhodeev, N. A. Gippius, J. Kuhl, and H. Giessen, Phys. Rev. Lett. **91**, 183901 (2003).
[9] E. Moreno, L. Martín-Moreno, and F. J. García-Vidal, J. Opt. A, Pure Appl. Opt. **8**, S94 (2006).
[10] U. Schröter and D. Heitmann, Phys. Rev. B **58**, 15419 (1998).
[11] J. A. Porto, F. J. García-Vidal, and J. B. Pendry, Phys. Rev. Lett. **83**, 2845 (1999).
[12] H. F. Schouten, T. D. Visser, D. Lenstra, and H. Blok, Phys. Rev. E **67**, 036608 (2003).
[13] K. H. Park, H. J. Eom, and T. J. Park, IEEE Trans. Antennas Propag. **42**, 286 (1994).
[14] A. Yu. Nikitin, F. López-Tejeira, and L. Martín-Moreno, Phys. Rev. B **75**, 035129 (2007).
[15] K. Uchida, IEEE Trans. Microwave Theory Tech. **35**, 481 (1987).